

Deep Smart Contract Intent Detection

Youwei Huang¹, Sen Fang², Jianwen Li^{1,3}, Jiachun Tao⁴, Bin Hu⁵, and Tao Zhang^{6*}

¹ Institute of Intelligent Computing Technology, Suzhou, CAS, China

² North Carolina State University, USA

³ Beijing Normal University - Hong Kong Baptist University United International College, China

⁴ Suzhou City University, China

⁵ Institute of Computing Technology, Chinese Academy of Sciences, China

⁶ Macau University of Science and Technology, Macao SAR

huangyw@iict.ac.cn, tazhang@must.edu.mo

*Corresponding author

Abstract—In recent years, researchers in the software security field have focused on detecting vulnerabilities in smart contracts to avoid significant losses of crypto assets on the blockchain. Despite early successes in this domain, detecting developers' intents in smart contracts is a more pressing issue, as malicious intents have resulted in substantial financial losses. Unfortunately, existing research lacks effective methods for detecting development intents in smart contracts.

To address this gap, we propose SMARTINTENTNN (Smart Contract Intent Neural Network), a deep learning model designed to automatically detect development intent in smart contracts. SMARTINTENTNN utilizes a pre-trained sentence encoder to generate contextual representations of smart contract code, a K-means clustering model to identify and highlight prominent intent features, and a bidirectional LSTM-based deep neural network for multi-label classification.

We trained and evaluated SMARTINTENTNN on a dataset comprising over 40,000 real-world smart contracts, employing self-comparison baselines in our experimental setup. The results demonstrate that SMARTINTENTNN achieves an F1-score of 0.8633 in identifying intents across 10 distinct categories, outperforming all baselines and filling the gap in smart contract detection by incorporating intent analysis.

Index Terms—Web3 Software Engineering, Smart Contract, Intent Detection, Deep Learning

I. INTRODUCTION

Web3, a term first coined by Gavin Wood¹ within the Ethereum ecosystem [1]–[3], refers to a decentralized network where applications, known as Decentralized Applications (DApps), run on blockchain infrastructure [4]–[7]. Web3 enables DApps to operate in a trustless environment by leveraging blockchain's immutable and distributed ledger technology. A smart contract, which serves as the backbone of DApp development, is defined as a computer program and transaction protocol designed to automatically execute, control, or document legally relevant events and actions based on the terms of a contract or agreement [8]–[10].

However, similar to other computer programs, smart contracts are susceptible to exploitation. They are exposed to vulnerabilities that hackers can exploit, as well as to malicious intents from developers aiming to defraud users. We categorize these risks into two types: external and internal. External risks

arise from attacks outside the smart contract, typically involving hackers exploiting vulnerabilities. In contrast, internal risks stem from malicious code intentionally designed and embedded by developers inside the smart contracts.

What are external risks? When considering smart contracts as computer programs, the primary external risks stem from the exploitation of vulnerabilities [11]. A notable example is the infamous DAO attack, triggered by a *reentrancy vulnerability* [12], [13], in which an attacker repeatedly invoked a function before the previous execution completed, enabling unauthorized withdrawals. Another common issue is *unchecked exceptions* [14]–[16], where improper error handling leads to unexpected contract behavior. Additionally, *integer overflow/underflow* [17] can cause arithmetic operations to wrap around, leading to incorrect account balances or infinite loops. More vulnerabilities in smart contracts have been comprehensively summarized by *Chu et al.* [18]. These external risks are attacks from outside the smart contract that exploit its vulnerabilities.

```
function changeTax(
    uint8 buyTax,
    uint8 sellTax
) public onlyOwner {
    _buyTax = buyTax;
    _sellTax = sellTax;
}

function setupEnableTrading() public onlyOwner {
    tradingEnabled = true;
}

function setupDisableTrading() public onlyOwner {
    tradingEnabled = false;
}

function teamUpdateLimits(
    uint256 newBalanceLimit,
    uint256 newSellLimit,
    uint256 newBuyLimit
) public onlyOwner {
    balanceLimit = newBalanceLimit;
    sellLimit = newSellLimit;
    buyLimit = newBuyLimit;
}
```

Fig. 1. Examples of a smart contract with malicious intents. BSC address: 0xDDa7f9273a092655a1cF077FF0155d6400ccE2A.

What are internal risks? In legal contracts, malicious

¹<https://gavwood.com>

terms can lead to significant losses for users. Similarly, in smart contracts, which are transaction protocols designed by developers, harmful terms can be embedded in the form of computer code. Our investigation reveals that, in recent years, an increasing number of risks have been intentionally injected by smart contract developers or DApp creators [19]–[22]. Malicious DApps purposely inject tricks and backdoors in their smart contracts to misappropriate users’ funds [23].

As illustrated in Fig. 1, several examples of internal risks in a smart contract are shown. In these examples, all functions include the *onlyOwner* modifier, which centralizes control in the hands of the contract owner. For instance, by adding the *onlyOwner* modifier to the *changeTax* function, the development team can arbitrarily change the tax fee for asset swaps. Similarly, *teamUpdateLimits* with the *onlyOwner* modifier allows developers to modify transaction limits. The other two functions are even more concerning, as they allow the owner to directly enable or disable trading within the smart contract. We define these risks, stemming from developers’ intents, as internal or intentional risks.

Our research focuses on detecting internal risks in smart contracts by identifying developers’ intent embedded within the code. There is already a substantial body of successful research dedicated to analyzing external risks, particularly in smart contract vulnerability detection [18]. However, few studies address internal risks, and no existing methods can detect developers’ intent from the context of smart contract code. Currently, the only way to identify such intents is through expert manual audits, which are time-consuming and costly [24]. This gap in the detection of unsafe developer intents motivates our research.

We present SMARTINTENTNN, a deep learning model comprising three key components: a Universal Sentence Encoder (USE) [25] for contextual representation of smart contracts, a trained K-means clustering model [26], [27] to highlight distinct intent, and a bidirectional long short-term memory (BiLSTM) network [28], [29] for multi-label classification. SMARTINTENTNN is implemented using TensorFlow.js [30], [31] and can detect ten categories of intents (see Table I).

We trained and evaluated SMARTINTENTNN on a dataset of over 40,000 labeled smart contracts, comparing it against self-comparison baselines, including classic LSTM [28], BiLSTM [29], CNN [32] models, and generative large language models (LLMs) such as GPTs [33]. SMARTINTENTNN achieved an *F1-score* of 0.8633, *accuracy* of 0.9647, *precision* of 0.8873, and *recall* of 0.8406, surpassing all baselines.

Our contributions can be summarized as follows:

- To the best of our knowledge, this is the first study to propose an approach for detecting developer intents behind smart contracts using deep learning models.
- We compiled a comprehensive dataset of over 40,000 labeled smart contracts, covering 10 categories of development intents.
- We provide a website for SMARTINTENTNN, with all documentation, code, dataset, and models available at <https://github.com/web3se-lab/web3-sekit>.

II. MOTIVATION

Why is it essential to identify the developers’ intent in smart contract development? – For the love of money is the root of all evil. In traditional web software development, the concept of developers’ intent is rarely discussed, as these applications are typically released by a trustworthy and centralized entity. These conventional applications generate revenue by providing high-quality software services to users and do not rely on their cryptocurrency systems. The entities behind these applications are responsible for the code logic and ensuring the software’s overall quality.

In stark contrast, Web3 applications are decentralized and financially driven, allowing any developer to deploy a smart contract and promote it to users for financial purposes. More critically, smart contracts in Web3 applications often include their economic systems, which are tied to real-value cryptocurrencies (e.g., Bitcoin). This is where potential risks emerge: as a smart contract accrues significant value², unscrupulous developers may exploit preset malicious code to steal or misappropriate users’ cryptocurrency.

Given the decentralized nature and the immense financial stakes involved in DApp development, understanding and scrutinizing the intent of developers becomes crucial. Without such scrutiny, users are at a heightened risk of falling victim to malicious activities that can lead to substantial financial losses.

Did developers’ malicious intent cause financial damage?

According to the 2022 Crypto Crime Report by Chainalysis [34], cryptocurrency scammers have stolen approximately \$7.8 billion worth of cryptocurrency from victims, with over \$2.8 billion resulting from rug pulls. A rug pull occurs when developers invoke malicious functions embedded in smart contracts to perform unfair transactions, such as illegally withdrawing funds or unpairing liquidity pools to misappropriate crypto assets [35], [36]. Compared to data from 2020, the losses in 2021 surged by 82%. Further investigation by HONEYBADGER revealed that 690 honeypot smart contracts accumulated more than \$90,000 in profit for their creators [19].

Most users are not programming experts and cannot audit the underlying code of these smart contracts, making them easy targets for malicious schemes like rug pulls, honeypots, and phishing scams. In the following sections, we will further detail and categorize the various potential malicious intents we have identified. These malicious actions by developers have caused and will continue to cause irreversible financial damage to users. Therefore, there is an urgent need for effective detection measures to identify and expose these unsafe intents in Web3 development.

Why do we propose an automated approach for detecting intent in smart contracts? Users need protection against smart contracts that conceal unsafe intents to prevent these intents from evolving into real harmful actions. Developers, on the other hand, often engage in practices like code cloning, reuse, and integrating third-party libraries during

²A way to estimate the value of a smart contract is to calculate its TVL, referring to <https://academy.binance.com/en/glossary/total-value-locked-tvl>.

Web3 development, which can inadvertently introduce risky third-party code. An automated detection tool aids developers in identifying and avoiding such intents, ensuring the integrity and security of their projects.

From a cost perspective, traditional security audits for smart contracts are manually performed by experts, making them time-consuming and costly. Although existing research has introduced automated methods for analyzing smart contracts, these primarily focus on vulnerabilities or scams [18]–[20]. An automated intent detection approach can significantly reduce the time, labor, and costs associated with security auditing. This motivates us to propose an automated method for detecting intents in smart contracts, thereby effectively reducing auditing costs and enhancing overall security.

III. BACKGROUND

In this section, we provide essential background knowledge, covering smart contracts with malicious intents, sentence embedding techniques, and bidirectional LSTMs.

A. Malicious Smart Contract Intent

Smart contracts facilitate online interactions via blockchain networks, and Ethereum, the most widely used smart contract platform, serves as an illustrative example of how developers with malicious intents can exploit these contracts to steal users' funds. Ethereum and similar blockchain platforms function as transaction-based systems, where both deploying and invoking smart contracts require transactions. Users are represented by externally owned accounts (EOAs), which are necessary for paying gas fees in ether (ETH), Ethereum's valuable native cryptocurrency.

As illustrated in Fig. 2, both developers and users maintain EOAs. A developer writes a smart contract, compiles it to bytecode executable on the Ethereum Virtual Machine (EVM) [37], and deploys it by signing a transaction with their private key, generating a unique contract address. Malicious developers might incorporate a *reward* function into the smart contract to lure users, prompting them to stake ETH in exchange for incentives such as NFTs (non-fungible tokens) [38].

A user might send a transaction to invoke a *deposit* function, paying 10 ETH to the smart contract address. Afterward, the user attempts to invoke the *reward* function to receive NFTs. However, if the developer has secretly implemented a *withdraw* function, they can steal the user's 10 ETH immediately. Once these transactions are confirmed on the blockchain, they cannot be altered or traced back, and the stolen funds are irretrievable.

B. Sentence Embedding

Embedding, also known as distributed representation [39], is a technique for learning dense representations of entities such as words, sentences, and images. Compared to word-level embeddings like word2vec [40] and GloVe [41], the Universal Sentence Encoder (USE) provides sentence-level embeddings by aggregating word representations within a sentence [42].

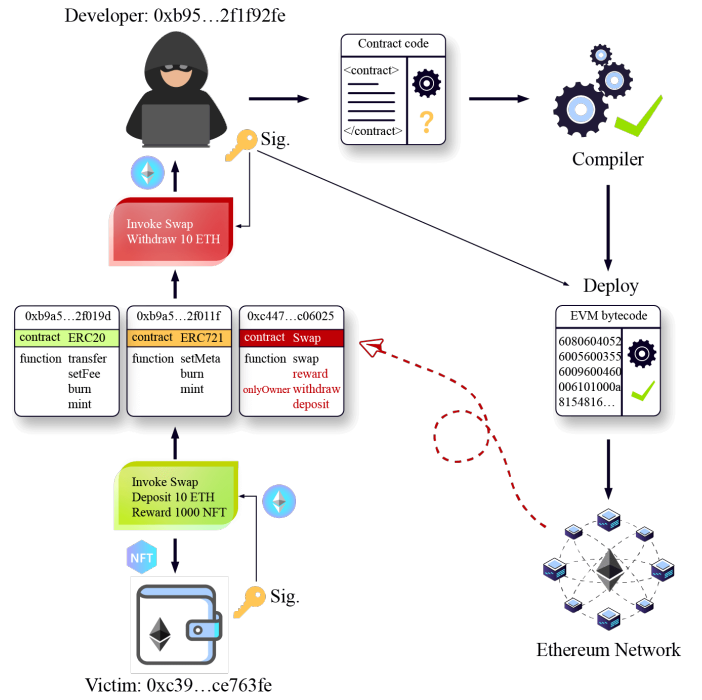


Fig. 2. A description of how developers exploit smart contracts to illegally benefit at the expense of users, detailing the process of creating and deploying contracts with malicious intents.

USE takes a sentence as input and outputs a contextual representation, ensuring that similar sentences are close in the generated vector space [39], [43]. In this paper, we treat every *function* snippet in a smart contract as a sentence and pass it into USE to obtain the corresponding contextual representation.

There are two main designs for USE. The first design is based on the transformer architecture [44], targeting high accuracy but at the cost of greater model complexity and resource consumption. The second design aims for efficient inference with slightly reduced accuracy by utilizing a deep averaging network (DAN) [45].

C. Bidirectional LSTM

A common LSTM cell is composed of a memory cell, a forget gate, an input gate, and an output gate [28]. The memory cell retains values over arbitrary time intervals, while the gates regulate the flow of information into and out of the cell. A bidirectional LSTM (BiLSTM) [29] incorporates two LSTM layers: one processes the input sequence in the forward direction and the other processes it in the backward direction. The output of a BiLSTM is the concatenation of the outputs from these two layers.

Compared to a standard LSTM, which only learns context dependency from the left side of the input sequence, a BiLSTM can learn dependencies from both sides of the input sequence. This bidirectional capability makes BiLSTM significantly more effective in understanding semantic contexts than a unidirectional LSTM.

IV. DATASET

To train and evaluate SMARTINTENTNN, we compiled an extensive dataset of over 40,000 smart contracts from the Binance Smart Chain (BSC) explorer³. BSC is an Ethereum-compatible blockchain, enabling smart contracts on BSC to also operate on Ethereum. Fig. 3 illustrates the data collection and preprocessing workflow.

Initially, we downloaded a substantial number of open-source smart contracts from the blockchain explorer. Then, we merged smart contracts containing multiple files and removed redundant or noisy code snippets. Finally, we employed regular expressions (RegEx) to extract code snippets based on Solidity syntax elements, generating a structured smart contract code tree.

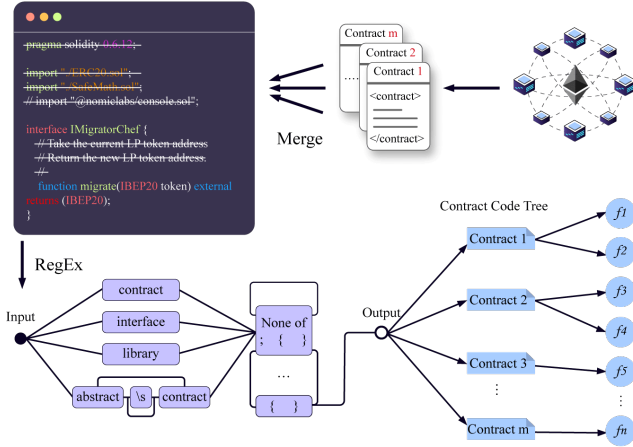


Fig. 3. Dataset preprocessing steps: (i) download open-source smart contracts from the BSC blockchain and label them; (ii) merge and clean the source code; (iii) generate the smart contract code tree.

A. Intent Labels

The dataset comprises ten categories of unsafe intents, as detailed in Table I. These labeling data were compiled from StaySafu⁴, along with the expertise of DApp developers and auditors.

TABLE I
CATEGORIES OF RISKY INTENTS

Id	Intent	Percentage	Instance
1	Fee	26.86%	<code>setFeeAddress(address)</code>
2	DisableTrading	5.34%	<code>enableTrading(bool)</code>
3	Blacklist	3.82%	<code>require(!isBlacklisted(sender))</code>
4	Reflect	37.50%	<code>tokenFromReflection(uint256)</code>
5	MaxTX	13.76%	<code>setMaxTxPercent(uint256)</code>
6	Mint	8.53%	<code>mint(uint256)</code>
7	Honeypot	0.23%	<code>require(allow[from])</code>
8	Reward	3.37%	<code>updateDividendTracker(address)</code>
9	Rebase	0.53%	<code>LogRebase(uint256, uint256)</code>
10	MaxSell	0.05%	<code>setMaxSellToken(uint256)</code>

The ten categories of intents in Table I are described below:

- 1 **Fee**: Arbitrarily changes transaction fees, directing them to specified wallet addresses.
- 2 **DisableTrading**: Enables or disables trading actions within a smart contract.
- 3 **Blacklist**: Restricts specified users' activities, potentially infringing on their trading rights.
- 4 **Reflect**: Redistributes transaction fees to holders based on their holdings, often used to incentivize holding native tokens.
- 5 **MaxTX**: Limits the maximum number or volume of transactions allowed.
- 6 **Mint**: Issues new tokens, potentially in an unlimited or controlled manner.
- 7 **Honeypot**: Traps user-provided funds by falsely promising to release funds while keeping the user's funds inaccessible.
- 8 **Reward**: Provides users with crypto assets as rewards to encourage token use, often regardless of the actual value of the rewards.
- 9 **Rebase**: Adjusts the total supply of tokens algorithmically to stabilize or change the token's price.
- 10 **MaxSell**: Limits the amount or frequency of token sales for specified users to restrict liquidity.

Each of these intents can appear multiple times in a smart contract. Our statistical analysis revealed that the most frequent intent is **Reflect**, appearing in 33,268 instances out of over 40,000 smart contracts, accounting for 37.5% of all intents. This is followed by **Fee** at 26.86% and **MaxTX** at 13.76%. The intent with the least occurrence is **MaxSell**, appearing in only 68 instances and accounting for a mere 0.05% of our dataset. These statistics indicate a higher prevalence of certain risks, such as **Reflect**, **Fee**, and **MaxTX**, in smart contracts on the BSC.

B. Code Cleaning

The source code of smart contracts on BSC exists in two forms: single-file and multi-file. A single-file contract has its `import` contracts merged by developers using a flattener tool before uploading. For multi-file contracts, we merge all files into a single document. We remove the Solidity compiler version specification (`pragma`), `import` statements, and `comments`, as `pragma` does not convey any developer's intent, `comments` do not affect intent implementation, and `import` statements are redundant after merging contracts.

C. Smart Contract Code Tree

Smart contracts, being composed of code, cannot be directly fed into a neural network. To prepare the input data, we create a Smart Contract Code Tree (CCTree). The CCTree organizes the smart contract source code into three layers: (i) the root layer, representing the entire smart contract document; (ii) the contract layer, representing the `contract` classes within the smart contract; (iii) the function layer, representing the `function` contexts within each `contract` class. The root layer contains a single node, denoted by **T**. The second layer lists the `contract` classes (e.g., `contract`, `interface`, `library`, `abstract`

³<https://bscscan.com>

⁴<https://www.staysafu.org>

contract), denoted by \mathcal{C} . The third layer includes leaf nodes with code snippets associated with keywords such as *function*, *event*, *modifier*, and *constructor*, denoted by \mathcal{F} . This structure allows systematic access to code data for model training and evaluation.

V. APPROACH

In this section, we present a DNN-based approach leveraging the SMARTINTENTNN model for detecting development intents in smart contracts. As illustrated in Fig. 4, SMARTINTENTNN consists of three core components. First, smart contract embedding using the USE converts the contract context into embedding vectors. Next, the intent highlight model with a K-means model emphasizes features with strong intents. Finally, we feed the highlighted data into a BiLSTM-based DNN layer to learn the representations of smart contracts and perform multi-label classification. A detailed explanation of our approach is provided in the following subsections.

A. Smart Contract Embedding

To generate contextual representations of a smart contract, we begin by considering each *function* within it. Each *function* is individually encoded, and these *function* embeddings are then combined to create a holistic representation of the smart contract.

$$\Phi(\mathcal{F}) : \mathcal{F} \rightarrow \mathbf{f} \quad (1)$$

Using the CCTree introduced in Section IV, an exhaustive traversal of all leaf nodes is performed. Consequently, each *function* (denoted as \mathcal{F} , referring to a leaf node) in a smart contract is transformed into a sentence embedding using the pre-trained USE based on the DAN. This embedding process is encapsulated by Formula 1, where Φ represents the contextual encoder, \mathcal{F} is the *function* context, and \mathbf{f} is the resulting *function* embedding vector.

To generate a sentence embedding for \mathcal{F} , the DAN model proceeds as follows:

$$\mathbb{T}(\mathcal{F}) : \mathcal{F} \rightarrow \mathbf{W}^{\mathcal{F}} = \{w_1, w_2, \dots, w_n\} \quad (2)$$

$$\phi(w_i) : w_i \rightarrow \mathbf{w}_i, \quad \mathbf{w}_i \in \mathbf{W}^{\mathcal{F}} \quad (3)$$

$$\mathbf{f}^0 = \frac{1}{n} \sum_{i=1}^n \mathbf{w}_i \quad (4)$$

The series of operations from Formula 2 to Formula 4 represents the initial step in the DAN model, termed “tokenizing”. Here, \mathbb{T} in Formula 2 transforms a sentence into word-level tokens. The text within *function* \mathcal{F} is dissected into an ordered set of word tokens $\mathbf{W}^{\mathcal{F}} = \{w_i\}_{i=1}^n$. Subsequently, ϕ in Formula 3 converts these tokens into word embeddings $\{\mathbf{w}_1, \mathbf{w}_2, \dots, \mathbf{w}_n\}$. Following this, Formula 4 computes the average of all word embedding vectors to yield \mathbf{f}^0 .

Deep feed-forward neural networks help learn increasingly abstract representations of input data with each layer [46].

Therefore, in the second step of the DAN model, the mean output \mathbf{f}^0 undergoes further enhancement through multiple feed-forward layers. Assuming n feed-forward layers, each layer can be represented by Formula 5, where \mathbf{W}_i is a weight matrix $\in \mathbb{R}^{k \times k}$ (with k representing the dimension of vector \mathbf{f}^i), σ is the activation function (e.g., sigmoid or tanh), and \mathbf{b}_i is the bias term.

$$\mathbf{f}^i = \sigma(\mathbf{W}_i \cdot \mathbf{f}^{i-1} + \mathbf{b}_i), \quad i \in \{1, 2, \dots, n\} \quad (5)$$

In the final step, \mathbf{f}^n is fed into a softmax layer, generating a universal representation of the *function* \mathcal{F} . Here, \mathbf{W}_s is a weight matrix $\in \mathbb{R}^{m \times k}$, where the input size is k , and the output is a *function* embedding vector with m features. Formula 6 produces \mathbf{f} , which embeds the context of the *function*.

$$\mathbf{f} = \text{softmax}(\mathbf{W}_s \cdot \mathbf{f}^n + \mathbf{b}_s) \quad (6)$$

These operations are applied to each *function* in a smart contract. The resulting embedding vectors \mathbf{f} are assembled into a matrix \mathbf{X} , which represents the entire smart contract, where $\mathbf{X} \in \mathbb{R}^{n \times m}$. Here, n corresponds to the number of *functions* in the smart contract, while m represents the dimension of \mathbf{f} .

B. Intent Highlight

Feeding \mathbf{X} directly into a DNN may fail to capture all of the developer’s specific intents in a smart contract. Thus, we introduce an intent highlight model to emphasize intent-related *functions*. This model employs K-means clustering to predict the intent strength of each vector \mathbf{f} in \mathbf{X} . By calculating intent strength, we enhance the features of vectors that strongly reflect the developer’s intent. This mechanism is illustrated by the formula $\mathbf{X}' = \mathbb{H}(\mathbf{X})$, where \mathbb{H} denotes the K-means-based intent highlight model, and \mathbf{X}' is the output of the intent-highlighted data.

To find the appropriate k value for K-means clustering, we compute the occurrence rate of each *function* \mathcal{F} within a randomly selected subset of the entire smart contract dataset. This subset, \mathbf{S} , consists of m smart contracts, denoted as $\mathbf{S} = \{\mathbf{T}_i\}_{i=1}^m$. The occurrence rate, $\mathbb{R}(\mathcal{F})$, is defined as the frequency with which a *function* appears in the subset, as detailed in Formula 7. If a *function* \mathcal{F} exists within the smart contract tree \mathbf{T}_i , it is counted as $\mathbb{I}\{\mathcal{F} \in \mathbf{T}_i\}$. We specifically tally the number of \mathcal{F} *functions* whose occurrence rate $\mathbb{R}(\mathcal{F}) > \rho$, where ρ is an experimentally determined threshold. The total count of these high-frequency *functions* gives us the value of k .

$$\mathbb{R}(\mathcal{F}) = \frac{1}{m} \sum_{i=1}^m \mathbb{I}\{\mathcal{F} \in \mathbf{T}_i\} \quad (7)$$

We compute the cosine distance between their embedding vectors when comparing the similarity of two documents [47]. Consider two *functions* (\mathcal{F}_A and \mathcal{F}_B) with embedding vectors

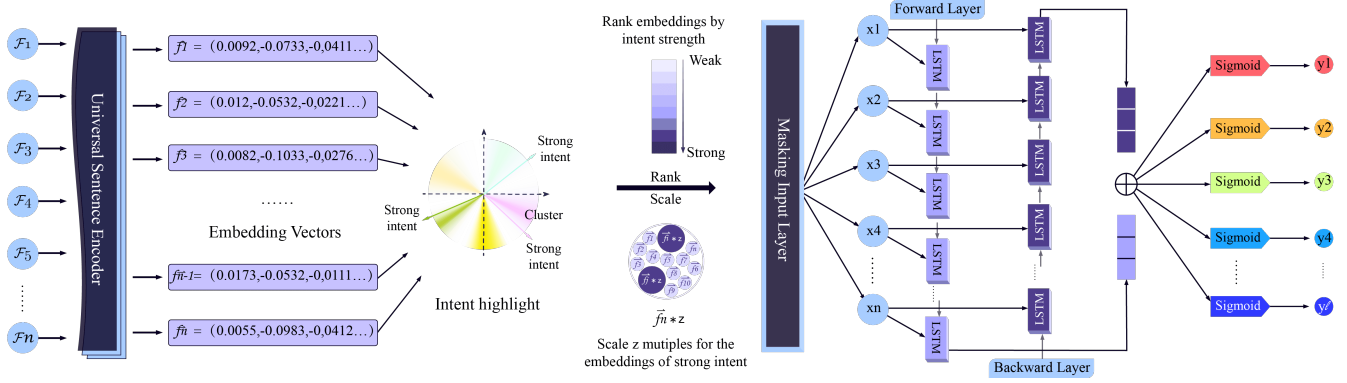


Fig. 4. Overview of the SMARTINTENTNN workflow: (i) encode smart contracts through the Universal Sentence Encoder; (ii) identify and highlight features of developers' distinct intents in smart contracts using a K-means model; (iii) feed the intent-highlighted data into a DNN for learning the representations of smart contracts. The architecture of our DNN includes an input layer, a BiLSTM layer, and a dense layer to output the multi-label binary classification results.

$\mathbf{f}^A = [f_1^A, f_2^A, \dots, f_n^A]$ and $\mathbf{f}^B = [f_1^B, f_2^B, \dots, f_n^B]$. Formula 8 calculates the text similarity between \mathcal{F}_A and \mathcal{F}_B , which is the cosine value of \mathbf{f}^A and \mathbf{f}^B . We use Formula 9 to transform cosine similarity into cosine distance.

$$\cos \langle \mathbf{f}^A, \mathbf{f}^B \rangle = \frac{\mathbf{f}^A \cdot \mathbf{f}^B}{\|\mathbf{f}^A\| \|\mathbf{f}^B\|} \quad (8)$$

$$D(\mathbf{f}^A, \mathbf{f}^B) = 1 - \cos \langle \mathbf{f}^A, \mathbf{f}^B \rangle \quad (9)$$

To identify the centroids for K-means clustering, we start with a training dataset $\{f'_i\}_{i=1}^n$, where each f'_i is an embedding vector representing a *function* \mathcal{F} from the previously described subset S . We initialize k random centroids $\{c_j^t\}_{j=1}^k$ for $t = 0, 1, \dots, z$, where z is the maximum number of iterations. K-means iteratively updates centroids by minimizing the cosine distance, as opposed to the original Euclidean distance. Each *function* embedding f'_i is assigned to the closest centroid c_j^t , forming a set M_j^t for each centroid. The centroid c_j^{t+1} is updated based on the weighted average of all vectors in M_j^t , as shown in Formula 10.

$$c_j^{t+1} = \frac{\sum_{f'_i \in M_j^t} f'_i}{|M_j^t|} \quad (10)$$

The objective is to minimize the total within-cluster variation (TWCV), as depicted in Formula 11. If f'_i belongs to M_j^t , the cosine distance is calculated. Here, $D(f'_i, c_j^t)$ represents the cosine distance between the *function* vector f'_i and the centroid c_j^t at iteration t .

$$\min_{t=0}^z \sum_{j=1}^k \sum_{f'_i \in M_j^t} D(f'_i, c_j^t) \quad (11)$$

After each iteration, the centroid c_j^t is updated to c_j^{t+1} . The training process continues until t reaches the maximum number of iterations, z , or the reduction in TWCV becomes negligible. Ultimately, this process identifies the most appropriate centroids $\{c_j\}_{j=1}^k$ for K-means.

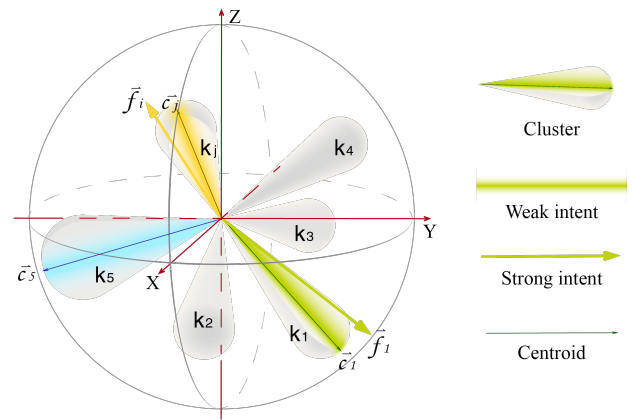


Fig. 5. A 3D coordinate system illustrating the principle of intent highlighting. The larger the vector angle deviates from the centroid, the stronger its intent.

Once the K-means model has been trained, we can input any *function* embedding vector f_i to calculate its within-cluster distance. Around the centroids c_j in Fig. 5, we observe some frequently occurring and similar *function* code snippets. Their vectors cluster densely around the centroids. These code snippets typically originate from public libraries, mainstream algorithms, or widely reused *functions*, indicating weak developer intent. In contrast, centroid-outlying *functions* are distinctive and express strong intent. Therefore, we consider the within-cluster distance as a measure of intent strength.

$$H_\mu(\mathbf{X}) = \mathbf{X} \odot (1 + (\mu - 1) \cdot \mathbb{I}\{D(f_i, c_j) \geq \lambda\}) \quad (12)$$

We scale f_i in \mathbf{X} by the predicted within-cluster distance to generate a new matrix $\mathbf{X}' \in \mathbb{R}^{n \times m}$. In Formula 12, $i \in \{1, 2, \dots, n\}$ and $j \in \{1, 2, \dots, k\}$, where λ is a distance threshold and μ is the scaling factor applied to f_i if its within-cluster distance $D(f_i, c_j) \geq \lambda$. These steps are illustrated in the middle part of Fig. 4 near the intent highlight model.

C. Multi-label Classification

In this section, we introduce the final part of Fig. 4, which involves using a DNN for multi-label classification. The architecture of the DNN comprises three layers: an input layer, a BiLSTM layer, and an output layer. We input the intent-highlighted data, represented by the matrix \mathbf{X}' produced by the previous intent highlight model, into the DNN.

Initially, the data is fed into the input layer, which accepts a sequence of $\mathbb{R}^{p \times m}$. Here, p corresponds to the number of functions \mathcal{F} input at each timestep, and m represents the dimensionality of each function embedding \mathbf{f}_i . For instance, USE outputs a vector of 512 dimensions, then $m = 512$. The row size of \mathbf{X}' may vary depending on the number of functions present in each smart contract. In cases where the number of rows in \mathbf{X}' is less than p , additional rows are padded with zero vectors. This input layer also functions as a masking layer, allowing TensorFlow to skip over these padded timesteps by setting the masking value to zero [48].

Next, the data flows into the BiLSTM layer, which also accepts a $\mathbb{R}^{p \times m}$ matrix, denoted by $\mathbf{X}'' = [\mathbf{f}_i]_{i=1}^p$, output from the input layer. Each LSTM layer in the BiLSTM contains p memory cells, thus there are a total of $2p$ cells when considering both forward and backward layers. Each row vector \mathbf{f}_i from \mathbf{X}'' is input into corresponding cells in both the forward and backward layers.

$$G_i^f = \alpha(\mathbf{W}_i^f \mathbf{f}_i + \mathbf{U}_i^f \mathbf{h}_{i-1} + \mathbf{b}_i^f) \quad (13)$$

$$G_i^u = \alpha(\mathbf{W}_i^u \mathbf{f}_i + \mathbf{U}_i^u \mathbf{h}_{i-1} + \mathbf{b}_i^u) \quad (14)$$

$$G_i^o = \alpha(\mathbf{W}_i^o \mathbf{f}_i + \mathbf{U}_i^o \mathbf{h}_{i-1} + \mathbf{b}_i^o) \quad (15)$$

$$\tilde{\Theta}_i = \beta(\mathbf{W}_i^\theta \mathbf{f}_i + \mathbf{U}_i^\theta \mathbf{h}_{i-1} + \mathbf{b}_i^\theta) \quad (16)$$

$$\Theta_i = G_i^f \odot \Theta_{i-1} + G_i^u \odot \tilde{\Theta}_i \quad (17)$$

$$\mathbf{h}_i = G_i^o \odot \gamma(\Theta_i) \quad (18)$$

Formulas 13 to 18 illustrate the computation process after a row vector \mathbf{f}_i is input into an LSTM cell, where $i \in \mathbb{N}^+$ and $i \leq p$. Here, Θ denotes the cell state vector, and $\tilde{\Theta}$ signifies the cell input activation vector. The initial state Θ_0 is initialized as a zero vector with a dimensionality of h (hidden units per LSTM cell). The various gates within the LSTM cell are represented as follows: G_i^f is the forget gate, G_i^u is the update (or input) gate, and G_i^o is the output gate. The weight matrices $\mathbf{W} \in \mathbb{R}^{h \times m}$ and $\mathbf{U} \in \mathbb{R}^{h \times h}$, along with the bias vector $\mathbf{b} \in \mathbb{R}^h$, are parameters learned during the training phase. The activation functions denoted by α , β , and γ can be tanh or sigmoid. The hidden state vector \mathbf{h}_i , which is also the output of the LSTM cell, has a dimensionality of h , with the initial hidden state \mathbf{h}_0 being initialized as a zero vector. The operator \odot denotes the Hadamard product (element-wise product) [49].

In a bidirectional LSTM, the forward layer generates \mathbf{h}_p^f , while the backward layer produces \mathbf{h}_p^b . The final output of the BiLSTM is obtained by concatenating these two vectors: $\mathbf{h} = \mathbf{h}_p^f \oplus \mathbf{h}_p^b$ [50].

The output of the BiLSTM layer is subsequently passed to the output layer, a multi-label binary classification dense layer, which accepts the vector \mathbf{h} of size $2h$.

$$\mathbf{y} = \text{sigmoid}(\mathbf{W}_c \mathbf{h} + \mathbf{b}) \quad (19)$$

In Formula 19, binary classification for each category (label) is performed using a sigmoid activation function. The weight matrix $\mathbf{W}_c \in \mathbb{R}^{l \times 2h}$, where $2h$ is the size of input vector \mathbf{h} and l is the number of target labels. The final output is a vector $\mathbf{y} = [y_1, y_2, \dots, y_l]$, where each element indicates the probability of the respective intent category. For each element y_i , a threshold is applied: $y_i \geq 0.5$ is set to 1, and $y_i < 0.5$ is set to 0. This results in a multi-hot vector, where ‘1’ indicates the presence and ‘0’ indicates the absence of an intent. This completes the intent detection process for a smart contract.

VI. EVALUATION

This section outlines the datasets and parameter configurations used in our experiments. We then describe the evaluation metrics and baselines applied. Finally, we present three research questions to comprehensively evaluate our proposed approach.

A. Dataset & Parameter Configurations

The dataset is divided into a training set and an evaluation set, each comprising 10,000 smart contracts. Specifically, the first 10,000 rows are utilized for training, while the rows from 20,000 to 29,999 are used for evaluation. The intermediate rows are reserved for potential extended training or evaluation in future experiments.

The training batch size is set to 50 smart contracts, resulting in a total of 200 batches to cover the 10,000 training samples. The models are trained over 100 epochs. The model is compiled using the ‘‘adam’’ optimizer and the ‘‘binaryCrossentropy’’ loss function. LSTM models are configured with 64 hidden units for single layers and 128 units for two-layered BiLSTM models, a configuration determined optimal based on preliminary experiments. The dimension of the output multi-hot vector \mathbf{y} , as described in Section V.C, is 10, corresponding to the ten categories of intent we aim to detect.

For intent highlighting using K-means clustering, the initial number of clusters k was set to 19, based on an occurrence rate threshold of $\rho = 0.75$. During training, empty clusters and identical centroids were merged or deleted, refining the number of clusters to 16. A distance threshold $\lambda = 0.21$ was used, with a maximum iteration count set to 80.

B. Evaluation Metrics

To evaluate the performance of our model, we utilize the confusion matrix [51] and derive several key metrics from it:

- **True Positive (TP):** The number of correctly predicted intent categories that exist in smart contracts.
- **True Negative (TN):** The number of correctly predicted non-existing intent categories in smart contracts.

- **False Positive (FP):** The number of incorrectly predicted intent categories that are falsely identified as existing in smart contracts.
- **False Negative (FN):** The number of intent categories that exist but are incorrectly predicted as non-existing in smart contracts.

Using the values of **TP**, **TN**, **FP**, and **FN**, we compute the following metrics: *accuracy*, *precision*, *recall*, and *F1-score* (*F1*) as defined in Equations 20-23.

$$\text{accuracy} = \frac{\text{TP} + \text{TN}}{\text{TP} + \text{FP} + \text{FN} + \text{TN}} \quad (20)$$

$$\text{precision} = \frac{\text{TP}}{\text{TP} + \text{FP}} \quad (21)$$

$$\text{recall} = \frac{\text{TP}}{\text{TP} + \text{FN}} \quad (22)$$

$$\text{F1} = \frac{2 \times \text{precision} \times \text{recall}}{\text{precision} + \text{recall}} \quad (23)$$

Accuracy is a fundamental metric that indicates the proportion of correct predictions over the total number of predictions. *Precision* measures the proportion of true positive predictions among all positive predictions made. *Recall* assesses the proportion of true positive predictions over all actual positive cases in the dataset. *F1-score* is the harmonic mean of *precision* and *recall*, providing a single metric that balances both concerns.

C. Baselines

As our study is the first to focus on smart contract intent detection, there are no prior works or experimental results available for direct comparison. To address this issue, we perform self-comparisons with several baselines, including classic models such as a basic LSTM model [28], a BiLSTM model [29], and a CNN model [32]. Additionally, we compare our model against advanced generative large language models (LLMs) from OpenAI⁵, specifically GPT-3.5-turbo and GPT-4o-mini, making our evaluation more comprehensive.

We implemented several variants of SMARTINTENTNN to conduct ablation studies. These variants include an intent highlight model with a scaling factor $\mu = 2$, as well as a version without the intent highlight model. Additionally, we replaced BiLSTM with LSTM in certain experimental setups.

D. Research Questions

We pose three research questions (RQs) to comprehensively evaluate our proposed approach:

- **RQ1:** How effectively does SMARTINTENTNN detect intents in smart contracts compared to the baselines?
- **RQ2:** How does intent highlight contribute to the performance of SMARTINTENTNN?
- **RQ3:** How effective is SMARTINTENTNN in detecting different categories of intents?

The above RQs are formulated to analyze from various aspects of SMARTINTENTNN. RQ1 evaluates its overall performance compared to established baselines. RQ2 investigates the specific contribution of the intent highlight model through ablation test. RQ3 examines its effectiveness across different categories of intents. Next, we will analyze and address these RQs based on the results and visualizations obtained from our evaluation experiments.

Firstly, we analyze RQ1. Figure 6 presents a trend chart of the evaluation metrics as the model is evaluated with 10,000 smart contracts. The metrics **AC**, **PR**, and **RE** represent *accuracy*, *precision*, and *recall*, respectively. It is observed that after approximately 7,344 evaluations, these metrics stabilize. Therefore, the metrics evaluated on 10,000 smart contracts are deemed reasonable and reliable. Finally, SMARTINTENTNN achieves an *F1-score* of 0.8633, *accuracy* of 0.9647, *precision* of 0.8873, and *recall* of 0.8406, corresponding to the first row of Table II, which represents the best-performing variant of SMARTINTENTNN.

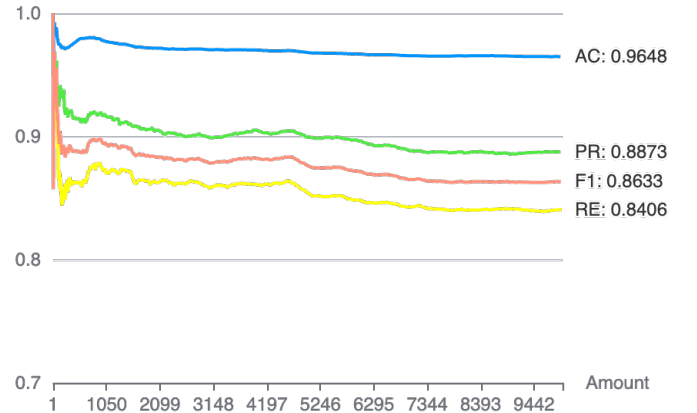


Fig. 6. Evaluation metrics trend of SMARTINTENTNN

We further analyze Table II to compare SMARTINTENTNN with its baseline models and ablation study variants. The evaluation results demonstrate that SMARTINTENTNN, incorporating the H_{16} ($\mu = 16$) intent highlight model and BiLSTM, significantly outperforms all ablation study variants and comparative benchmarks. Notable improvements in the *F1-score* include: 28.14% over LSTM, 14.79% over BiLSTM, 27.80% over CNN, 83.64% over GPT-3.5-turbo, and 63.26% over GPT-4o-mini. Furthermore, ablation tests reveal that SMARTINTENTNN with a BiLSTM layer outperforms the single LSTM variant by 3.40% in *F1-score*, underscoring the advantage of BiLSTM in capturing contextual information from both past and future data, thus enabling a better understanding of the semantic structure for more accurate intent classification.

Specifically, SMARTINTENTNN outperforms LLM baselines because LLMs, such as OpenAI's GPTs, are designed for general-purpose tasks. Although they possess strong generalization capabilities, they lack the fine-tuning required for the

⁵<https://openai.com>

TABLE II
BASELINES COMPARISON

Model	Accuracy	Precision	Recall	F1-score
SMARTINTENTNN (Ablation Test)				
USE-H₁₆-BiLSTM	0.9647	0.8873	0.8406	0.8633
USE-H ₂ -BiLSTM	0.9581	0.8438	0.8386	0.8412
USE-H ₁₆ -LSTM	0.9581	0.8731	0.7999	0.8349
USE-BiLSTM	0.9524	0.8337	0.8003	0.8167
USE-LSTM	0.9478	0.8319	0.7587	0.7936
Baseline Models				
LSTM	0.9172	0.7725	0.5973	0.6737
BiLSTM	0.9320	0.7871	0.7200	0.7521
CNN	0.9093	0.6922	0.6596	0.6755
GPT-3.5-turbo	0.8375	0.4135	0.5447	0.4701
GPT-4o-mini	0.7821	0.3703	0.9240	0.5288

specific domain of smart contract intent detection. In contrast, SMARTINTENTNN is explicitly trained for this task, enabling it to capture and understand the contextual semantics of the code and the specific intents of the developers. Therefore, surpassing LLMs is an expected outcome.

Answer to RQ1 ▶ By utilizing a USE pre-trained model, a K-means-based intent highlight model, and a BiLSTM-based multi-label classification DNN, SMARTINTENTNN can effectively detect and classify ten types of unsafe development intents in smart contracts, outperforming classic deep learning models and cutting-edge LLMs.

Secondly, we analyze RQ2. The intent highlight model identifies and emphasizes distinctive *functions* with strong intents through K-means clustering. As shown in Fig. 7, Subfigure (a) displays all clusters, where each of the 16 clusters represents a common *function*'s spatial centroid. Subfigure (b) focuses on one cluster, where hexagons mark centroids, circles represent *functions* with weaker intents, and stars highlight *functions* with stronger intents. Edges between nodes indicate within-cluster distances, illustrating intent strength. Subfigure (c) highlights various *functions*, with red labels identifying those with strong intents, such as *setFees* and *setTxLimitExempt*. While these highlighted *functions* may not be inherently malicious, they are distinctive enough to be emphasized. The vector features of these *functions* are then scaled by a factor of μ to enhance learning in subsequent DNN layers.

From Table II, it is clear that SMARTINTENTNN variants incorporating the intent highlight model offer substantial performance improvements. Specifically, with LSTM, the variant using intent highlight model H₁₆ ($\mu = 16$) shows a 5.20% gain in *F1-score* over its non-highlight counterpart. Similarly, for BiLSTM variants, introducing H₂ ($\mu = 2$) results in a 3.00% increase, and this improvement escalates to 5.71% with $\mu = 16$. These findings confirm the substantial impact of the intent highlight model in improving performance.

Answer to RQ2 ▶ The intent highlight model markedly enhances SMARTINTENTNN's performance in intent detection by amplifying features of *functions* with prominent intents, making the learning process more robust and accurate.

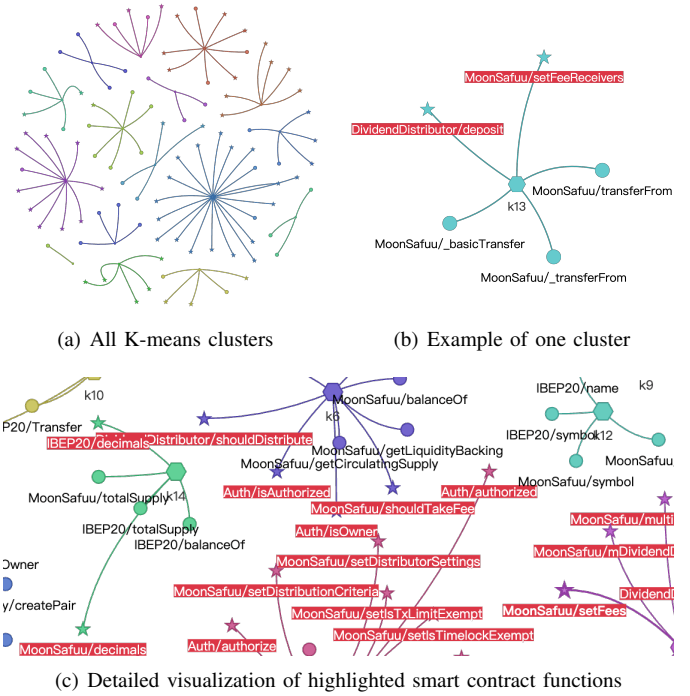


Fig. 7. Visualization of the Intent Highlight Model

Finally, we analyze RQ3. As shown in Fig. 8, the radar chart illustrates the performance metrics for ten distinct intent categories. Specifically, red circles represent the *F1-score*, green diamonds indicate the *precision*, yellow triangles denote the *recall*, and blue rectangles signify the *accuracy*. The ten axes on the radar chart correspond to the ten different intent categories. From the chart, we find that the performance of SMARTINTENTNN in detecting different categories of intents varies.

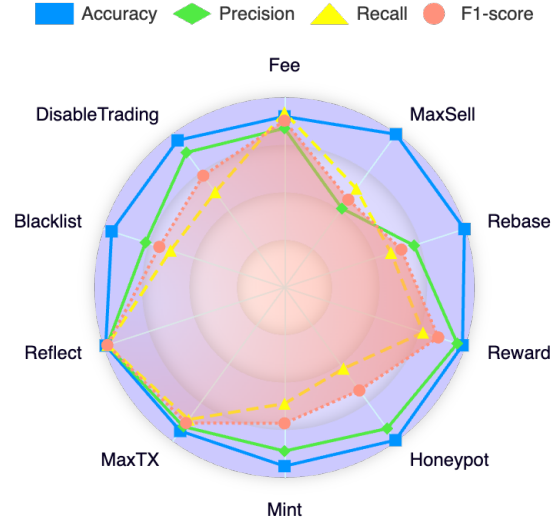


Fig. 8. Evaluation metrics of SMARTINTENTNN for different intents.

From the radar chart, it is evident that three intents, **Reflect**,

MaxTX, and **Fee**, achieve the highest *F1-scores*, with values of 0.98, 0.88, and 0.87 respectively, demonstrating outstanding detection performance. Conversely, the *F1-score* for **MaxSell** is the lowest at 0.57, indicating relatively poor performance in detecting this intent. This discrepancy can be attributed to the imbalance in our dataset. The proportion of **Reflect**, **MaxTX**, and **Fee** intents is significantly higher, allowing the model to be more effectively trained on these categories. In contrast, **MaxSell** samples constitute only 0.05% of the dataset, leading to insufficient training and consequently lower detection performance.

Answer to RQ3 ▶ SMARTINTENTNN exhibits varying effectiveness in detecting different intent categories. Although detection is weaker for certain intents, the overall accuracy for each category remains high, exceeding 90%, underscoring the model’s efficacy in distinguishing intent presence or absence. As data collection becomes more balanced, the model’s performance across different intents is expected to equalize.

VII. THREATS TO VALIDITY

A. Internal Validity

A major threat to the internal validity of our study is the dataset imbalance. For example, the **MaxSell** intent constitutes only 0.05% of our dataset, considerably less than other intent labels. This scarcity could limit our model’s ability to accurately identify this intent. To address this, we employ techniques such as oversampling, undersampling, and cross-validation to mitigate the imbalance. However, the natural rarity of these intents reflects their real-world prevalence, suggesting proportionately lower associated risks. Additionally, SMARTINTENTNN is designed to be continuously trainable; as we gather more data on these rarer intents, we will retrain and fine-tune the model to improve detection performance. Despite these measures, the detection of less frequent intents like **MaxSell** remains less effective, but this mirrors their limited impact in practical scenarios.

B. External Validity

The principal challenge to the external validity of our model stems from the diversity of programming languages used for smart contract development. Primarily trained on Solidity, the most popular smart contract programming language [52], our model effectively covers a vast majority of real-world smart contracts. While our current model does not yet extend to other languages (e.g., Vyper [53] and JavaScript), the adaptability of SMARTINTENTNN allows it to be retrained with additional data to support these languages. For bytecode-only contracts, deploying decompilers to convert the bytecode to source code allows the model to predict intents based on the contextual semantics embedded in the contracts. By virtue of its continuous retraining capability, SMARTINTENTNN maintains robustness and effectiveness, ensuring it can adapt to the evolving landscape of smart contract languages and effectively address external validity.

VIII. RELATED WORK

In this section, we review related work on external and internal risks and explain how our approach differentiates itself from previous studies.

A. External Risks

Traditional formal methods have significantly contributed to smart contract vulnerability detection. Tools like Oyente [14] and Mythril [54] use symbolic execution and control flow verification. Vandal [15] employs logical specifications for EVM bytecode analysis, while ZEUS [16] leverages abstract interpretation and symbolic model checking. SmartCheck [55] and Securify [56] utilize static analysis techniques. TEETHER [57] automates vulnerability identification and exploit generation directly from binary bytecode. Additional methods include sFuzz [58], which employs branch distance-driven fuzzing, Osiris [59], combining symbolic execution and taint analysis for integer error detection, Slither [60], which uses static analysis to convert smart contract code into an intermediate representation for vulnerability detection, and SMARTIAN [61], integrating static and dynamic analyses to effectively discover bugs in smart contracts. With the advancement of deep learning, detection efficiency and accuracy have improved. SaferSC [62] employs LSTM-based sequential learning, and ContractWard [63] uses machine learning for feature extraction. DR-GCN and TMP [64] integrate graph neural networks, while CGE [65] and AME [66] combine deep learning with expert patterns. ESCORT [67] uses multi-label classifiers and transfer learning, and DMT [68] enhances bytecode vulnerability detection. SCVHunter [69] utilizes heterogeneous graph attention networks, and Clear [70] leverages contrastive learning to significantly improve detection performance.

All the above methods focus on detecting vulnerabilities as external risks caused by development bugs. However, our work targets internal risks by detecting intentionally unsafe code, filling a gap in smart contract security study.

B. Internal Risks

Internal risks, with fewer studies, often result from developers’ malicious intent. Phishing scams have been investigated in several studies, including those by SIEGE [21] and DELight-GBM [71]. HONEYBADGER [19] exposes honeypots through symbolic execution, while FAIRCON [72] assesses contractual fairness in smart contracts. The “Trade or Trick” approach [23] employs machine learning techniques to detect scam tokens on the Uniswap platform. SCSGuard [20] targets scam detection in bytecode, specifically addressing Ponzi schemes and honeypots. More recent advances include TTG-SCSD [73], which employs topological data analysis for detecting smart contract scams, and CryptoScamTracker [74], which addresses cryptocurrency giveaway scams using certificate transparency logs. Pied-Piper [75] integrates datalog analysis with directed fuzzing to uncover backdoors in Ethereum ERC token contracts. Additionally, Tokeer [36] investigates rug pull risks by leveraging configurable transfer models.

Although these studies address various aspects of internal risks, such as phishing scams, rug pulls, and Ponzi schemes, none systematically define or detect a wide range of unsafe developer intents. In contrast, our study identifies ten specific negative intents and employs SMARTINTENTNN for comprehensive multi-label classification, offering a more robust solution to internal risk analysis.

IX. CONCLUSION

We have proposed SMARTINTENTNN, the first approach for detecting development intent in smart contracts. The model comprises a pre-trained USE model, an intent highlight model based on K-means clustering, and a DNN integrated with a BiLSTM layer. We trained and evaluated our model on a dataset of over 40,000 smart contracts, which were cleaned and labeled into ten distinct categories of intents. Experimental results demonstrate that our model surpasses all baselines, achieving an *accuracy* of 0.9647, a *precision* of 0.8873, a *recall* of 0.8406, and an *F1-score* of 0.8633. Our work fills a critical gap in smart contract security study by addressing developer intent detection.

REFERENCES

- [1] V. Buterin *et al.*, “A next-generation smart contract and decentralized application platform,” *white paper*, vol. 3, no. 37, pp. 2–1, 2014.
- [2] G. Wood *et al.*, “Ethereum: A secure decentralised generalised transaction ledger,” *Ethereum project yellow paper*, vol. 151, no. 2014, pp. 1–32, 2014.
- [3] A. M. Antonopoulos, *Mastering ethereum: Building smart contracts and dapps*. O’Reilly Media, Inc, 2018.
- [4] S. Nakamoto, “Bitcoin: A peer-to-peer electronic cash system,” *Decentralized Business Review*, p. 21260, 2008.
- [5] S. Porru, A. Pinna, M. Marchesi, and R. Tonelli, “Blockchain-oriented software engineering: challenges and new directions,” in *2017 IEEE/ACM 39th International Conference on Software Engineering Companion (ICSE-C)*. IEEE, 2017, pp. 169–171.
- [6] I. Bashir, *Mastering blockchain*. Packt Publishing Ltd, 2017.
- [7] Z. Zheng, S. Xie, H.-N. Dai, X. Chen, and H. Wang, “Blockchain challenges and opportunities: A survey,” *International journal of web and grid services*, vol. 14, no. 4, pp. 352–375, 2018.
- [8] N. Szabo, “Smart contracts: building blocks for digital markets,” *EXTROPY: The Journal of Transhumanist Thought*,(16), vol. 18, no. 2, p. 28, 1996.
- [9] W. Zou, D. Lo, P. S. Kochhar, X.-B. D. Le, X. Xia, Y. Feng, Z. Chen, and B. Xu, “Smart contract development: Challenges and opportunities,” *IEEE transactions on software engineering*, vol. 47, no. 10, pp. 2084–2106, 2019.
- [10] Ethereum Foundation, “Introduction to smart contracts,” 2024. [Online]. Available: <https://ethereum.org/en/developers/docs/smart-contracts>
- [11] D. He, Z. Deng, Y. Zhang, S. Chan, Y. Cheng, and N. Guizani, “Smart contract vulnerability analysis and security audit,” *IEEE Network*, vol. 34, no. 5, pp. 276–282, 2020.
- [12] B. Jiang, Y. Liu, and W. K. Chan, “Contractfuzzer: Fuzzing smart contracts for vulnerability detection,” in *Proceedings of the 33rd ACM/IEEE international conference on automated software engineering*, 2018, pp. 259–269.
- [13] L. Su, X. Shen, X. Du, X. Liao, X. Wang, L. Xing, and B. Liu, “Evil under the sun: Understanding and discovering attacks on ethereum decentralized applications,” in *30th USENIX Security Symposium (USENIX Security 21)*, 2021, pp. 1307–1324.
- [14] L. Luu, D.-H. Chu, H. Olickel, P. Saxena, and A. Hobor, “Making smart contracts smarter,” in *Proceedings of the 2016 ACM SIGSAC conference on computer and communications security*, 2016, pp. 254–269.
- [15] L. Brent, A. Jurisevic, M. Kong, E. Liu, F. Gauthier, V. Gramoli, R. Holz, and B. Scholz, “Vandal: A scalable security analysis framework for smart contracts,” *arXiv preprint arXiv:1809.03981*, 2018.
- [16] S. Kalra, S. Goel, M. Dhawan, and S. Sharma, “Zeus: analyzing safety of smart contracts.” in *Ndss*, 2018, pp. 1–12.
- [17] D. Perez and B. Livshits, “Smart contract vulnerabilities: Does anyone care?” *arXiv preprint arXiv:1902.06710*, pp. 1–15, 2019.
- [18] H. Chu, P. Zhang, H. Dong, Y. Xiao, S. Ji, and W. Li, “A survey on smart contract vulnerabilities: Data sources, detection and repair,” *Information and Software Technology*, vol. 159, p. 107221, 2023.
- [19] C. F. Torres, M. Steichen *et al.*, “The art of the scam: Demystifying honeypots in ethereum smart contracts,” in *28th USENIX Security Symposium (USENIX Security 19)*, 2019, pp. 1591–1607.
- [20] H. Hu, Q. Bai, and Y. Xu, “Scsguard: Deep scam detection for ethereum smart contracts,” in *IEEE INFOCOM 2022-IEEE Conference on Computer Communications Workshops (INFOCOM WKSHPS)*. IEEE, 2022, pp. 1–6.
- [21] S. Li, R. Wang, H. Wu, S. Zhong, and F. Xu, “Siege: Self-supervised incremental deep graph learning for ethereum phishing scam detection,” in *Proceedings of the 31st ACM International Conference on Multimedia*, 2023, pp. 8881–8890.
- [22] J. Zhou, T. Jiang, H. Wang, M. Wu, and T. Chen, “Dapphunter: Identifying inconsistent behaviors of blockchain-based decentralized applications,” in *2023 IEEE/ACM 45th International Conference on Software Engineering: Software Engineering in Practice (ICSE-SEIP)*. IEEE, 2023, pp. 24–35.
- [23] P. Xia, H. Wang, B. Gao, W. Su, Z. Yu, X. Luo, C. Zhang, X. Xiao, and G. Xu, “Trade or trick? detecting and characterizing scam tokens on uniswap decentralized exchange,” *Proceedings of the ACM on Measurement and Analysis of Computing Systems*, vol. 5, no. 3, pp. 1–26, 2021.
- [24] Binance Academy, “What is a smart contract security audit?” 2023. [Online]. Available: <https://academy.binance.com/en/articles/what-is-a-smart-contract-security-audit>
- [25] D. Cer, Y. Yang, S.-y. Kong, N. Hua, N. Limtiaco, R. S. John, N. Constant, M. Guajardo-Cespedes, S. Yuan, C. Tar *et al.*, “Universal sentence encoder,” *arXiv preprint arXiv:1803.11175*, 2018.
- [26] J. MacQueen, “Classification and analysis of multivariate observations,” in *5th Berkeley Symp. Math. Statist. Probability*, 1967, pp. 281–297.
- [27] K. Krishna and M. N. Murty, “Genetic k-means algorithm,” *IEEE Transactions on Systems, Man, and Cybernetics, Part B (Cybernetics)*, vol. 29, no. 3, pp. 433–439, 1999.
- [28] S. Hochreiter and J. Schmidhuber, “Long short-term memory,” *Neural computation*, vol. 9, no. 8, pp. 1735–1780, 1997.
- [29] A. Graves and J. Schmidhuber, “Framewise phoneme classification with bidirectional lstm and other neural network architectures,” *Neural networks*, vol. 18, no. 5-6, pp. 602–610, 2005.
- [30] M. Abadi, P. Barham, J. Chen, Z. Chen, A. Davis, J. Dean, M. Devin, S. Ghemawat, G. Irving, M. Isard *et al.*, “Tensorflow: a system for large-scale machine learning,” in *12th USENIX symposium on operating systems design and implementation (OSDI 16)*, 2016, pp. 265–283.
- [31] D. Smilkov, N. Thorat, Y. Assogba, C. Nicholson, N. Kreeger, P. Yu, S. Cai, E. Nielsen, D. Soegel, S. Bileschi *et al.*, “Tensorflow.js: Machine learning for the web and beyond,” *Proceedings of Machine Learning and Systems*, vol. 1, pp. 309–321, 2019.
- [32] Y. LeCun, Y. Bengio *et al.*, “Convolutional networks for images, speech, and time series,” *The handbook of brain theory and neural networks*, vol. 3361, no. 10, p. 1995, 1995.
- [33] J. Achiam, S. Adler, S. Agarwal, L. Ahmad, I. Akkaya, F. L. Aleman, D. Almeida, J. Altenschmidt, S. Altman, S. Anadkat *et al.*, “Gpt-4 technical report,” *arXiv preprint arXiv:2303.08774*, 2023.
- [34] Chainalysis, “The 2022 crypto crime report,” Chainalysis Inc., Tech. Rep., 2022. [Online]. Available: <https://go.chainalysis.com/2022-Crypto-Crime-Report.html>
- [35] Binance Academy, “Rug pull,” 2024. [Online]. Available: <https://academy.binance.com/en/glossary/rug-pull>
- [36] Y. Zhou, J. Sun, F. Ma, Y. Chen, Z. Yan, and Y. Jiang, “Stop pulling my rug: Exposing rug pull risks in crypto token to investors,” in *Proceedings of the 46th International Conference on Software Engineering: Software Engineering in Practice*, 2024, pp. 228–239.
- [37] Ethereum Foundation, “Ethereum Virtual Machine (EVM),” 2024. [Online]. Available: <https://ethereum.org/en/developers/docs/evm/>
- [38] Q. Wang, R. Li, Q. Wang, and S. Chen, “Non-fungible token (nft): Overview, evaluation, opportunities and challenges,” *arXiv preprint arXiv:2105.07447*, 2021.
- [39] T. Mikolov, I. Sutskever, K. Chen, G. S. Corrado, and J. Dean, “Distributed representations of words and phrases and their composi-

- tionality,” *Advances in neural information processing systems*, vol. 26, 2013.
- [40] K. W. Church, “Word2vec,” *Natural Language Engineering*, vol. 23, no. 1, pp. 155–162, 2017.
- [41] J. Pennington, R. Socher, and C. D. Manning, “Glove: Global vectors for word representation,” in *Proceedings of the 2014 conference on empirical methods in natural language processing (EMNLP)*, 2014, pp. 1532–1543.
- [42] R. Kiros, Y. Zhu, R. R. Salakhutdinov, R. Zemel, R. Urtasun, A. Torralba, and S. Fidler, “Skip-thought vectors,” *Advances in neural information processing systems*, vol. 28, 2015.
- [43] T. Mikolov, K. Chen, G. Corrado, and J. Dean, “Efficient estimation of word representations in vector space,” *arXiv preprint arXiv:1301.3781*, 2013.
- [44] A. Vaswani, N. Shazeer, N. Parmar, J. Uszkoreit, L. Jones, A. N. Gomez, L. Kaiser, and I. Polosukhin, “Attention is all you need,” *Advances in neural information processing systems*, vol. 30, 2017.
- [45] M. Iyyer, V. Manjunatha, J. Boyd-Graber, and H. Daumé III, “Deep unordered composition rivals syntactic methods for text classification,” in *Proceedings of the 53rd annual meeting of the association for computational linguistics and the 7th international joint conference on natural language processing (volume 1: Long papers)*, 2015, pp. 1681–1691.
- [46] Y. Bengio, A. Courville, and P. Vincent, “Representation learning: A review and new perspectives,” *IEEE transactions on pattern analysis and machine intelligence*, vol. 35, no. 8, pp. 1798–1828, 2013.
- [47] F. Rahutomo, T. Kitasuka, and M. Aritsugi, “Semantic cosine similarity,” in *The 7th international student conference on advanced science and technology ICAST*, vol. 4, no. 1, 2012, p. 1.
- [48] TensorFlow Team, “Tensorflow.js api,” 2024. [Online]. Available: <https://js.tensorflow.org/api/latest/#layers.masking>
- [49] R. A. Horn and C. R. Johnson, *Matrix analysis*. Cambridge university press, 2012.
- [50] C. Faith and E. A. Walker, “Direct sum representations of injective modules,” *J. Algebra*, vol. 5, no. 2, pp. 203–221, 1967.
- [51] D. M. Powers, “Evaluation: from precision, recall and f-measure to roc, informedness, markedness and correlation,” *arXiv preprint arXiv:2010.16061*, 2020.
- [52] The Next Web, “These are the top 10 programming languages in blockchain,” May 2019. [Online]. Available: <https://thenextweb.com/news/javascript-programming-java-cryptocurrency>
- [53] V. Buterin, “Vyper documentation,” *Vyper by Example*, p. 13, 2018.
- [54] B. Mueller, “A framework for bug hunting on the ethereum blockchain,” *ConsenSys/mythril*, 2017.
- [55] S. Tikhomirov, E. Voskresenskaya, I. Ivanitskiy, R. Takhaviev, E. Marchenko, and Y. Alexandrov, “Smartcheck: Static analysis of ethereum smart contracts,” in *Proceedings of the 1st International Workshop on Emerging Trends in Software Engineering for Blockchain*, 2018, pp. 9–16.
- [56] P. Tsankov, A. Dan, D. Drachler-Cohen, A. Gervais, F. Buenzli, and M. Vechev, “Securify: Practical security analysis of smart contracts,” in *Proceedings of the 2018 ACM SIGSAC Conference on Computer and Communications Security*, 2018, pp. 67–82.
- [57] J. Krupp and C. Rossow, “teether: Gnawing at ethereum to automatically exploit smart contracts,” in *27th USENIX Security Symposium (USENIX Security 18)*, 2018, pp. 1317–1333.
- [58] T. D. Nguyen, L. H. Pham, J. Sun, Y. Lin, and Q. T. Minh, “sfuzz: An efficient adaptive fuzzer for solidity smart contracts,” in *Proceedings of the ACM/IEEE 42nd International Conference on Software Engineering*, 2020, pp. 778–788.
- [59] C. F. Torres, J. Schütte, and R. State, “Osiris: Hunting for integer bugs in ethereum smart contracts,” in *Proceedings of the 34th annual computer security applications conference*, 2018, pp. 664–676.
- [60] J. Feist, G. Grieco, and A. Groce, “Slither: a static analysis framework for smart contracts,” in *2019 IEEE/ACM 2nd International Workshop on Emerging Trends in Software Engineering for Blockchain (WETSEB)*. IEEE, 2019, pp. 8–15.
- [61] J. Choi, D. Kim, S. Kim, G. Grieco, A. Groce, and S. K. Cha, “Smartian: Enhancing smart contract fuzzing with static and dynamic data-flow analyses,” in *2021 36th IEEE/ACM International Conference on Automated Software Engineering (ASE)*. IEEE, 2021, pp. 227–239.
- [62] W. J.-W. Tann, X. J. Han, S. S. Gupta, and Y.-S. Ong, “Towards safer smart contracts: A sequence learning approach to detecting security threats,” *arXiv preprint arXiv:1811.06632*, 2018.
- [63] W. Wang, J. Song, G. Xu, Y. Li, H. Wang, and C. Su, “Contractward: Automated vulnerability detection models for ethereum smart contracts,” *IEEE Transactions on Network Science and Engineering*, vol. 8, no. 2, pp. 1133–1144, 2020.
- [64] Y. Zhuang, Z. Liu, P. Qian, Q. Liu, X. Wang, and Q. He, “Smart contract vulnerability detection using graph neural network,” in *IJCAI*, 2020, pp. 3283–3290.
- [65] Z. Liu, P. Qian, X. Wang, Y. Zhuang, L. Qiu, and X. Wang, “Combining graph neural networks with expert knowledge for smart contract vulnerability detection,” *IEEE Transactions on Knowledge and Data Engineering*, 2021.
- [66] Z. Liu, P. Qian, X. Wang, L. Zhu, Q. He, and S. Ji, “Smart contract vulnerability detection: from pure neural network to interpretable graph feature and expert pattern fusion,” *arXiv preprint arXiv:2106.09282*, 2021.
- [67] C. Sendner, H. Chen, H. Fereidooni, L. Petzi, J. König, J. Stang, A. Dmitrienko, A.-R. Sadeghi, and F. Koushanfar, “Smarter contracts: Detecting vulnerabilities in smart contracts with deep transfer learning,” in *NDSS*, 2023.
- [68] P. Qian, Z. Liu, Y. Yin, and Q. He, “Cross-modality mutual learning for enhancing smart contract vulnerability detection on bytecode,” in *Proceedings of the ACM Web Conference 2023*, 2023, pp. 2220–2229.
- [69] F. Luo, R. Luo, T. Chen, A. Qiao, Z. He, S. Song, Y. Jiang, and S. Li, “Scvhunter: Smart contract vulnerability detection based on heterogeneous graph attention network,” in *Proceedings of the IEEE/ACM 46th International Conference on Software Engineering*, 2024, pp. 1–13.
- [70] Y. Chen, Z. Sun, Z. Gong, and D. Hao, “Improving smart contract security with contrastive learning-based vulnerability detection,” in *Proceedings of the IEEE/ACM 46th International Conference on Software Engineering*, 2024, pp. 1–11.
- [71] W. Chen, X. Guo, Z. Chen, Z. Zheng, and Y. Lu, “Phishing scam detection on ethereum: Towards financial security for blockchain ecosystem,” in *IJCAI*, vol. 7, 2020, pp. 4456–4462.
- [72] Y. Liu, Y. Li, S.-W. Lin, and R. Zhao, “Towards automated verification of smart contract fairness,” in *Proceedings of the 28th ACM Joint Meeting on European Software Engineering Conference and Symposium on the Foundations of Software Engineering*, 2020, pp. 666–677.
- [73] S. Fan, S. Fu, Y. Luo, H. Xu, X. Zhang, and M. Xu, “Smart contract scams detection with topological data analysis on account interaction,” in *Proceedings of the 31st ACM International Conference on Information & Knowledge Management*, 2022, pp. 468–477.
- [74] X. Li, A. Yepuri, and N. Nikiforakis, “Double and nothing: Understanding and detecting cryptocurrency giveaway scams,” in *Proceedings of the Network and Distributed System Security Symposium (NDSS)*, 2023.
- [75] F. Ma, M. Ren, L. Ouyang, Y. Chen, J. Zhu, T. Chen, Y. Zheng, X. Dai, Y. Jiang, and J. Sun, “Pied-piper: Revealing the backdoor threats in ethereum erc token contracts,” *ACM Transactions on Software Engineering and Methodology*, vol. 32, no. 3, pp. 1–24, 2023.